Morphological and orientation studies of injection moulded nylon-6,6/Kevlar composites

Z. Yu, A. Ait-Kadi and J. Brisson*

CERSIM, Department of Chemical Engineering and Chemistry, Faculté des Sciences et de Génie, Université Laval, Québec G1K 7P4, Canada

(Received 14 January 1993; revised 9 June 1993)

In this work, nylon-6,6/Kevlar short fibre composites have been processed by injection moulding. Their microstructure, and fibre and matrix orientation, measured by wide-angle X-ray diffraction (WAXD), have been studied as a function of two major processing variables, i.e. the injection speed and the mould temperature. At low mould temperatures, skin, underskin and core structures have been observed, while at high mould temperatures only skin and core structures were found. Fibre orientation patterns exhibit both a processing and a geometrical dependence. Matrix orientation patterns are different from those of the pure polymer moulded material and are mainly influenced by the fibre orientations, which are themselves affected by the processing conditions.

(Keywords: injection moulding; orientation; nylon-6,6/Kevlar composites)

INTRODUCTION

Short-fibre-reinforced thermoplastics have recently received considerable attention in the field of composites, since they can be processed by using highly automated and comparatively economic processes, such as injection moulding.

The incorporation of fibres into a polymer matrix produces a microscopically inhomogeneous material (i.e. a composite), with structure and properties which are different from those of each component acting on its own. In the composite, the properties usually depend more on the processing technique and conditions than those of the polymer matrix in its unfilled form. The structural elements that are most sensitive to the processing history are fibre and matrix orientation, which have become among the most interesting topics in morphological studies of injection moulded composites. Although the morphological structure of composites produced by injection moulding has been intensively studied and reviewed by several authors[1-3], orientation of the matrix chains has not yet been well characterized. This is particularly true for semicrystalline polymer matrices where the fibre–matrix interactions may act through either transcrystallization of the matrix around the fibres or the formation of specific interactions, such as hydrogen bonds, between the fibres and the matrix.

Kevlar fibres are composed of highly oriented polyamides. Their outstanding mechanical properties and low gravity justify their use in high-technology composite applications. However, experience has shown that the adhesion of Kevlar to most thermoplastics is poor. Nylon-6,6 is also a polyamide and is one of the most widely used thermoplastic materials. In order to favour fibre/matrix interactions, the nylon-6,6/Kevlar composite system was chosen on account of the structural similarity of the fibres and the matrix. In previous studies, we have investigated the mechanical properties and the interface of nylon/Kevlar composites[4,5]. In this present paper, focus has been put on the influence of injection moulding parameters on the orientation behaviour of nylon-6,6 and Kevlar fibres in short-fibre-reinforced composites, which has a preponderant influence on the properties of the resulting parts.

A variety of methods have been developed to characterize the molecular orientation of polymers[6], among which the most widely used are birefringence, Fourier transform infra-red (*FT*i.r.) spectroscopy and X-ray diffraction. For composite systems such as the one being studied here, the birefringence technique is not particularly useful because of the difficulty involved in separating the contributions resulting from the two macroscopic phases, i.e. the fibres and the matrix, from the contributions of the crystalline and amorphous parts of the matrix. The presence of macroscopic domains also makes *FT*i.r. spectroscopy difficult to use.

Contact microradiography (CMR), which is used extensively for glass-fibre-reinforced thermoplastics[7], is not amenable to organic fibre studies because of the necessity to introduce a heavy element (usually Pb) into the fibres. Image analysis, which is widely used for composites[8-10], has been attempted previously[11]. However, Kevlar fibres are strong, flexible and abrasion resistant and do not yield fibre cross-sections with smooth boundaries after being polished using aluminium powder. Therefore, significant errors are introduced in the image analysis of the cross-sections.

The X-ray diffraction method is particularly useful to assess the orientation of the crystalline phase. This technique can be used to characterize the fibre orientation

* To whom correspondence should be addressed

0032-3861/94/07/1409-10

in composites provided that the fibres are crystalline and oriented. In such systems, other methods are often not applicable. For this study, X-ray diffraction was chosen to characterize the crystalline phase orientation of both fibre and matrix. Although there is some overlap in the diffraction peaks which belong to the fibre and the matrix, it is still possible, through careful selection of measured reflections, to study the orientation of each crystalline phase that is present. The orientation of the amorphous phase of the matrix has not been attempted because of the weakness of its main scattering peak, which lies under the most intense diffraction peaks in nylon-6,6.

The microstructure, and the fibre and matrix orientation of the injection moulded parts will be discussed in relationship to the main injection variables, which are mould temperature and injection speed. The final aim of this work is to allow a quantitative evaluation of orientation factors for use in the prediction of the mechanical properties of composite systems, with the latter being the subject of a separate paper.

EXPERIMENTAL

Nylon-6,6 (Zytel 103HS®), reinforced by short Kevlar fibres, with a fibre length of 6 mm and a fibre content of 35 wt%, was provided by Du Pont in the form of granules. These materials were dried in a CERCO-SEMIP air convection drier at 110°C for 48 h prior to their use in injection moulding.

Injection moulding of pure nylon-6,6 and the composite pellets was performed by using a NISSEI NC-8000PZ injection moulding machine with a maximum injection capacity of $152\,cm^3\,s^{-1}$, a maximum injection speed of $21.52\,m\,s^{-1}$, and a maximum pressure of 147 MPa. The injection parameters used are shown in *Table 1*. The samples were moulded according to ASTM D-638M specifications. In the text, the terms 'moulded parts' or 'moulded pieces' refer to injection moulded samples that have been prepared in accordance with this ASTM method. The terms 'head' and 'tail' zone of a moulded piece are defined as the two bell zones, and the 'front neck' and 'rear neck' zones refer, respectively, to the connection zones between the bone and the front and rear bells in a dumbbell-shaped moulded part, appearing in consecutive order along the mould filling direction. The term 'centre' refers to the longitudinal centre of the moulded piece. The different areas of the sample are represented schematically in *Figure 1*. For the sake of concision, the moulded pieces prepared under the various

Table 1 Injection moulding variables for nylon-6,6 and its Kevlar composites

	Nylon-6,6	Composite
Material temperature (°C)		
Rear	251	260
Centre	260	275
Front	271	290
Nozzle	279	290
Injection speed (% of maximum)[a]	10	90
Hold pressure (% of maximum)	95	95
Holding time (s)	35	35
Cooling time (s)	50	50
Screw speed (rpm)	80	80

[a] Values used for mould temperatures of 18 and 85°C

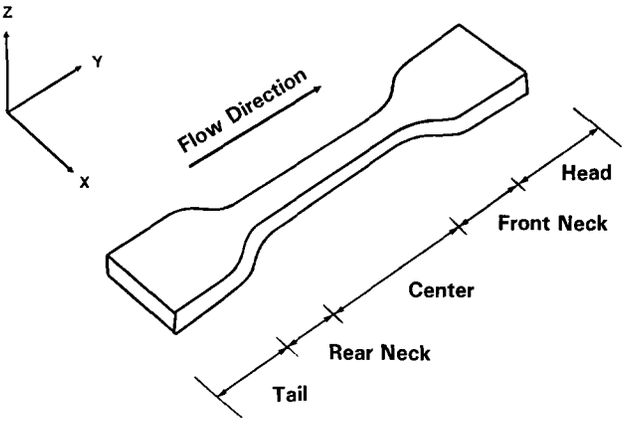

Figure 1 Designation of the sample areas used in this study

processing conditions are denoted as follows:

(a) LSLT = low injection speed, low mould temperature;
(b) HSLT = high injection speed, low mould temperature;
(c) LSHT = low injection speed, high mould temperature;
(d) HSHT = high injection speed, high mould temperature.

The microstructures of the injection moulded samples were observed through a Zeiss polarizing optical microscope. Prior to observation, the moulded parts were microtomed with a tungsten knife at liquid nitrogen temperature using a Reichert-Jung 2050 Supercut microtome. Each layer in a thickness of 15 μm were cut parallel to the *XY* or *YZ* planes of the sample (cf. *Figure 1*). The cut layers were held between two microscopic glass slides which had been saturated with glycerol to compensate for distortion. Observations were performed at ambient temperatures and the dimensions of each observed structure were measured using a micrometer eyepiece. Photographs were taken under polarized light.

Fibre and matrix orientation were measured using a Rigaku Rotaflex rotating anode generator (Model RU 200BH) with nickel-filtered CuKα radiation, operating at 55 kV and 190 mA. The skin layer of the samples used in the orientation studies was removed by using a diamond saw. Azimuthal scans of 002 ($2\theta = 13.7°$, *d*-spacing = 0.645 nm) reflection of the Kevlar fibres, and of 002 ($2\theta = 12.2°$, *d*-spacing = 0.640 nm) and 100 ($2\theta = 20.3°$, *d*-spacing = 0.436 nm) for nylon-6,6 were recorded at a scan speed of $5°\,min^{-1}$, for various sections of the moulded parts. Experimental curves were smoothed by using the Savitsky–Golay method[12] before calculations were made. The average intensity from each side of the diffraction peak of a θ–2θ scan of the samples placed at the azimuthal angle corresponding to that of the orientation scan was calculated and used as the background intensity in the evaluation of the orientation factors.

In cases where more than one diffraction plane contributed to the azimuthal scan, a deconvolution process was performed prior to calculation of the orientation factors. Each diffraction peak was simulated with a Pearson VII function:

$$I(\chi) = I[(1 + Z^2/m)]^{-m} \quad (1)$$

where $Z = (\chi_{1/2} - \chi_0)/\chi_{1/2}$. The $\chi_{1/2}$ term represents the width of the peak at mid-height, χ_0 is the azimuthal position of the peak, and m is an adjustable variable. All of the variables in this function were adjusted until the difference between the experimental curve and that plotted from the function was minimal. The orientation

factor was subsequently calculated from the deconvoluted curve.

The orientation factors are coefficients of a series of even-ordered Legendre polynomials $\langle P_n \cos\chi \rangle$, for $n=2$, 4, etc. These are usually abbreviated as $\langle P_n \rangle$, where the $\langle P_2 \rangle$ value is equivalent to the well-known Hermans' orientation factor. The observed orientation factors for a given reflection, $\langle P_n \cos\chi \rangle_o$, are calculated from the corrected diffraction curve, by using the following formula:

$$\langle P_n \cos\chi \rangle_o = \int_0^{\pi/2} I(\chi) P_n(\cos\chi) \sin\chi \, d\chi \Big/ \int_0^{\pi/2} I(\chi) \sin\chi \, d\chi \tag{2}$$

where $I(\chi)$ is the intensity at an azimuthal angle of χ. $\langle P_n \rangle$ would be equal to 0 for random orientation, to 1 for perfect orientation in the reference direction, and to -0.5 for perfect orientation perpendicular to the reference direction.

RESULTS AND DISCUSSION

Morphology of injection moulded composites

The existence of different morphologies at the surface of the sample moulded, which is termed the skin structure, and at the inner portion of the samples, or core structure, is well known for injection moulded thermoplastics. For short-fibre-reinforced thermoplastics, the classification of the different structures is based mainly on changes in the fibre orientation patterns. For thermoplastics, variation of the different structures in the composites is strongly dependent on the inherent properties of the polymer, on the processing conditions and on spatial location in the moulded part.

Three zones, which are termed skin, underskin and core structures, were observed for samples prepared at low mould temperatures, at both low and high injection speeds, as shown in *Figure 2a*, which is a photograph of a sample cut parallel to the *XZ* plane at a distance of 0.8 mm from the top surface. In the skin layer, fibres generally appear as grouped, dark circular or elliptical shadows. This corresponds to fibres oriented perpendicular or slightly inclined to the injection or flow direction. This observation is further confirmed by *Figure 3*, which shows a photograph taken in the *YZ* plane of the samples, where the fibres now clearly appear as continuous dark lines.

In the underskin structure, fibres are seen to preferentially orient in the flow direction, since they appear as elongated dark lines. In the core region, fibres still orient in the flow direction, although to a lesser extent than in the underskin. For high mould temperatures, only two zones are observed, corresponding to the skin and the core structures, as shown in *Figure 2b*. The fibre orientation behaviour in the two zones is similar to that of the low mould temperature samples.

This behaviour is noticeably different from that observed by Bright *et al.*[13] for short-glass-fibre-filled

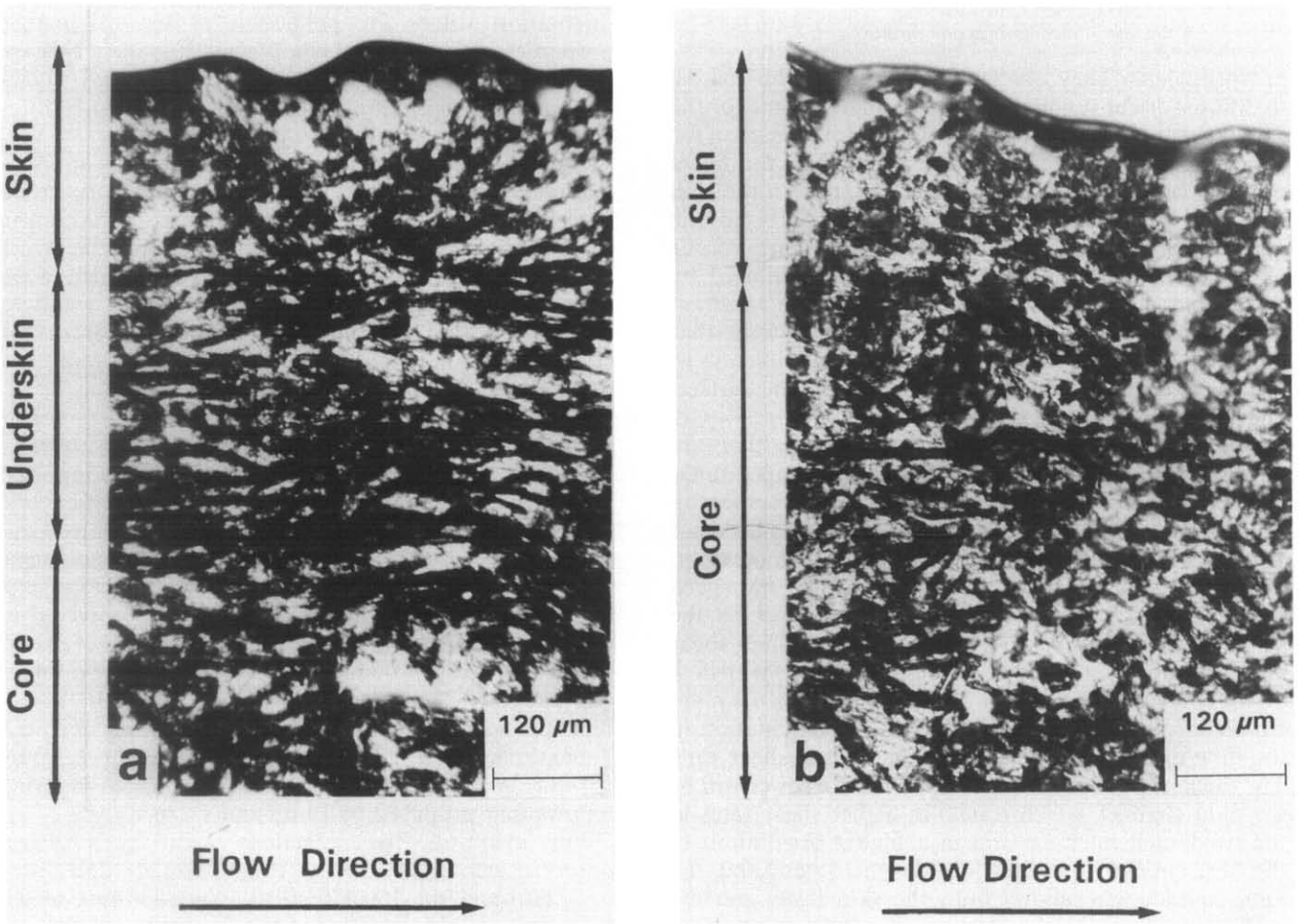

Figure 2 Polarized optical microscope photographs of sections of composites cut parallel to the *XZ* plane: (a) high speed, low temperature (HSLT) injection moulded sample and: (b) high speed, high temperature (HSHT) injection moulded sample

Figure 3 Polarized optical microscope photograph of the skin layer of a composite cut parallel to the *YZ* plane

Table 2 Characteristics of the microstructures of moulded composites produced under different injection moulding conditions

Microstructure	Fibre orientation	Structural thickness (mm)[a]			
		LSLT	HSLT	LSHT	HSHT
Skin	Random	0.20 ±0.04	0.18 ±0.03	0.17 ±0.07	0.16 ±0.05
Underskin	Parallel	0.46 ±0.03	0.38 ±0.01	–	–
Core	Partially parallel[b]	1.68	1.86	2.65	2.67

[a] Reported values represent the average for each sample: total thickness of the samples is constant (3.00±0.02 mm), and consists of one core, two underskin and two skin structures

[b] Parallel to the flow direction (injection direction)

polypropylene. They observed, at low injection speeds, that fibres orient randomly in the moulding plane for the skin layers but preferentially along the flow direction for the core structure. At high injection speeds, the fibres partially orient along the injection direction in the skin structure whereas they orient perpendicularly to the injection direction in the core structure. Furthermore, our observations are also different from those reported by Singh and Kamal[14]. They indicated, in the injection moulding of short-glass-fibre-filled polypropylene, that the fibres oriented preferentially in the flow direction at or very close to the surface, randomly near the surface, and transversely in the core.

The dimensions of the various structures that are observed are given in *Table 2*. At low mould temperatures, the dimensions of the skin and underskin structures in samples moulded at low injection speeds slightly decrease with injection speed. This is attributed to an increase in the mould wall–polymer contact time when the speed decreases, which leads to a thick solidified layer, i.e. the skin structure. This solidified layer creates a high shear flow field at the solid–melt interface. Such a shear flow orients the fibres in the flow direction, which is the main characteristic of the underskin structure. Orientation in the flow direction increases with increasing shear rate. The thicker the solidified skin layer, the narrower will be the fluid channel, which results in higher shear rates in the solid–melt interface and in a higher orientation of the fibres in the flow direction. On the other hand, the long contact time allows both the skin layer and the underskin structures to become 'frozen', resulting in thicker skin and underskin structures and in preservation of the fibre orientation patterns in these zones.

For high mould temperatures, the smaller temperature difference between the molten fluid and the mould temperature produces a thinner solidified layer, which will consequently orient less fibres in the flow direction, as can be inferred from the above discussion. In addition, such a small temperature difference is only capable of freezing the skin layer, which thus allows the underskin structure to be destroyed by the subsequently incoming melted polymer. The effect of injection speed on the thickness of the skin structure at high mould temperatures is similar to that observed for low mould temperatures.

Orientation measurement conditions

This present nylon-6,6/Kevlar composite system is not an easy one to characterize from the point of view of orientation. Both the matrix and the fibre are crystalline, and it is therefore imperative to carefully choose the reflections used for the orientation measurements, in order to avoid, as much as possible, any superimposition of various peaks of the polymers.

Generally speaking, in an injection moulded short-fibre composite, the fibre orientation is three-dimensional. However, in this study, due to the particular geometry of the mould used (the ratio of width/thickness varied from 10/1 to 2/1), and also to the length of the fibres, which has been estimated as being ~1 mm after injection moulding[15], fibre orientation is preferentially planar. This has been shown previously[11] and can also be inferred from the photographs of the composite sample morphology presented above. Furthermore, one of the objectives of this study is to provide quantitative orientation values for prediction of the mechanical properties of the moulded composites. For these types of calculations, uniaxial orientation factors are used. Therefore, uniaxial orientation measurements for both fibres and matrix were chosen for this study.

It must, however, be acknowledged that this approximation is itself a source of error, and further work would be necessary to fully quantify the orientation pattern in three dimensions. In order to partially limit the errors caused by this approach, and to gain a better idea of the three-dimensional order present in the samples, we chose to measure the orientation of as many axes of the crystalline phase unit cells as possible, all with respect to the flow direction.

Matrix orientation. The first extensive X-ray diffraction work on oriented fibres of nylon-6,6 was reported by Ecochard in 1946[16]. The following year, Bunn and Garner[17] published the first crystal structure investigation on nylon-6,6. As with many other polymers, nylon-6,6 is polymorphic. The most stable crystal structure, which was, in fact, the only one observed in this work, is called the α-form, and is composed of planar sheets of hydrogen-bonded molecules stacked on top of one another. The structure is triclinic with one repeat unit per unit cell, and has the following unit cell dimensions: $a=0.49$, $b=0.54$, c (fibre axis)$=1.72$ nm; $\alpha=48.5°$, $\beta=77°$ and $\gamma=63.5°$. In this work, our indexing follows that proposed by Bunn and Garner[17].

For nylon-6,6, the reflections with the strongest observed intensities are the 010+110 ($2\theta=25.3°$, $d=0.357$ nm) and the 100 ($2\theta=20.3°$, $d=0.436$ nm), which both lie on the equator, at a χ angle of 90°. A medium intensity reflection is also worth investigating, namely the 002 reflection which was observed at a 2θ

angle of 13.17° ($d=0.641$ nm) and at a χ value of 34°. Because of the triclinic unit cell, this reflection is not meridional, and the reciprocal-space axis, c^*, does not match the direction of the direct space axis, c. Nevertheless, the two latter reflections will be used for orientation measurements, since they allow the investigation of a specific reciprocal axis. Azimuthal scans of pure, well-oriented nylon-6,6 samples, taken at θ–2θ positions of the 100 and 002 reflections, are reported in *Figures 4a* and *4b*. In the case of the 100 reflection, a second, less intense reflection can also be seen as a shoulder centred at $\chi \sim 60°$. This reflection can be attributed to the 112 reflection, which appears at a d-spacing of 0.435 nm. Because of its weak intensity at this 2θ position, when compared to that of the 100 reflection, it is not easy to separate the contribution of this reflection from the total intensity contribution, particularly in the case where weak orientation occurs. Therefore, the intensity measurement has not been corrected for the presence of this weak reflection, which will result in a small, systematic underestimation of the orientation factor of this reciprocal axis.

Using any arbitrary reflection, it is possible to deduce the orientation of the c-axis by using the relationship proposed by Lovell and Mitchell[18]:

$$\langle P_n \rangle = \frac{\langle P_n \rangle_o}{P_n \cos \chi} \tag{3}$$

For a single meridional reflection where $\chi = 0°$, $\langle P_n \rangle = \langle P_n \rangle_o$, whereas for an equatorial reflection, $\langle P_n > = -0.5 \langle P_n \rangle_o$. This formula is suitable for our purposes providing that the denominator does not take a value of zero. In the case of $\langle P_2 \rangle$, this happens for an angle of 54.7°. Unfortunately, this value is too close to that of the azimuthal angle of the 002 reflection of nylon-6,6 (34°) to allow it to be used in this particular case. Therefore, for convenience, the $< P_2 >$ values of all of the reciprocal axes were used directly in this present study.

Azimuthal scans of pure Kevlar were taken at the $\theta - 2\theta$ positions of the 100 and 002 reflections of nylon-6,6, in order to determine possible overlaps, and are reported in *Figures 4c* and *4d*, respectively. For the orientation measurement of the nylon-6,6 matrix in the composites, the 100 reflection could not be used because of its superimposition with the strong 110 reflection of the Kevlar fibres. Therefore, only the 002 reflection was used to investigate the orientation of the matrix in the composite samples.

Fibre orientation. The fibre used in this study, i.e. Kevlar, is a highly oriented form of poly(*p*-phenylene terephthalamide) (PPTA). Northolt and Van Aartsen[19] have reported that the crystal structure of Kevlar is monoclinic, in fact pseudo-orthorhombic, with $a=0.787$,

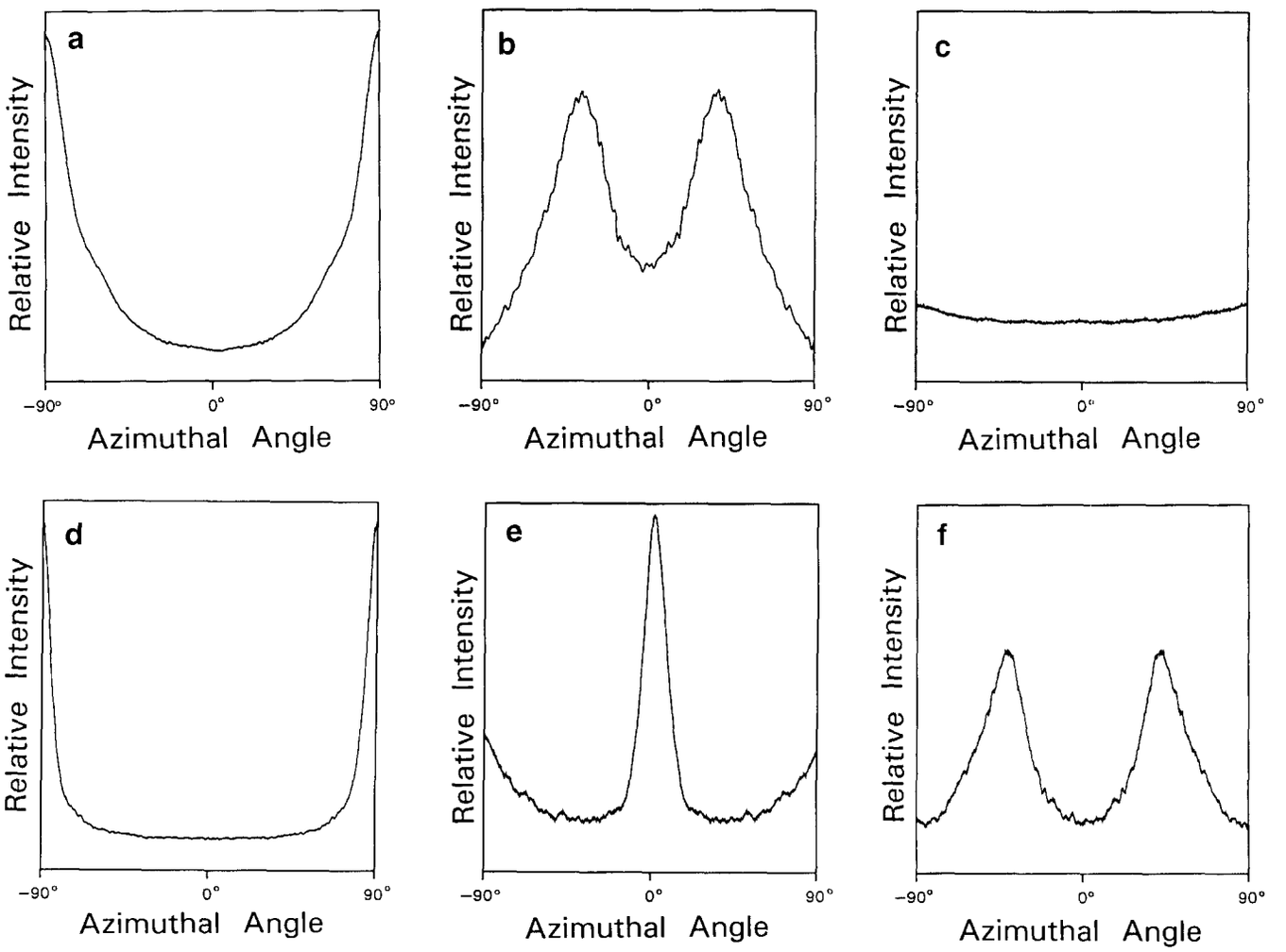

Figure 4 Azimuthal scans of well oriented nylon-6,6 and Kevlar fibres: (a) nylon-6,6 sample, 100 reflection ($2\theta=20.3°$); (b) nylon-6,6 sample, 002 reflection ($2\theta=12.2°$); (c) Kevlar fibres, nylon-6,6 100 position ($2\theta=20.3°$); (d) Kevlar fibres, nylon-6,6 002 position ($2\theta=12.2°$); (e) Kevlar fibres, 002 reflection ($2\theta=13.7°$); (f) nylon-6,6 sample, Kevlar 002 position ($2\theta=13.7°$)

$b=0.518$ and $c=1.290$ nm (fibre axis) and $\gamma=90°$. Two of the reflections have strong intensities, i.e. the 110 ($2\theta=20.5°$, $d=0.433$ nm) and the 006 ($2\theta=42.0°$, $d=0.215$ nm). The 002 reflection ($2\theta=13.7°$, $d=0.645$ nm) is of medium intensity. Because of the almost perfect orientation of Kevlar fibres ($\langle P_2\rangle$ is greater than 0.95), the orientation of the c-axis of the crystals will be used as the orientation of the fibres themselves in this work. The same approximation has been used by Lim and White[20] in a fibre orientation study of Kevlar–polycarbonate composites.

Since, in this study, the matrix is also crystalline, it is important to select Kevlar diffraction peaks which do not superimpose with those of the nylon-6,6 matrix. Pure Kevlar fibres and well-oriented nylon-6,6 samples (hot drawn at 150°C, draw ratio of 3.5) were scanned at various diffraction angles in order to determine reflection superimpositions. The 006 reflection superimposed with that of the 017 and 127 reflections of nylon-6,6, which appeared at approximately the same χ angle, whereas the $hk0$ reflections overlapped completely with the nylon-6,6 $hk0$ reflections. The 002 reflection was therefore selected, in spite of the fact that it was only of medium intensity. Its azimuthal scan, for a pure Kevlar fibre bundle, is shown in *Figure 4e*, where the maximum intensity is reached for $\chi=0°$. For the Kevlar $00l$ reflections, the $\langle P_2\rangle_o$ value is equal to the $\langle P_2\rangle$ value, since the χ angle is zero.

An azimuthal scan of pure, oriented nylon-6,6, taken at the diffraction position of the 002 reflection of Kevlar is shown in *Figure 4f*. A medium weak reflection appears at $\chi=34°$. This reflection is attributed to the (002) plane of nylon-6,6, which reaches its maximum intensity at a 2θ angle of 12.2°. However, because of crystal lattice defects, typical of polymeric materials, the width of the diffraction spots is such that a non-negligible intensity is still detectable at $2\theta=13.7°$, which is the position of the 002 reflection of Kevlar. This reflection is therefore expected to be observed in the azimuthal scans of the composites, particularly since nylon forms the bulk of the composite (65 wt%). It will, however, appear at the same χ angle in scans taken at 2θ angles of 12.2° and 13.7°, and can therefore be identified in this way.

Orientation of injection moulded unfilled nylon-6,6

Molecular orientation in pure injection moulded polymers has been the subject of many studies[21–23]. It is known that the molecular orientation arises from 'frozen' stress in the mould, which depends critically on the processing conditions. Due to the capacity limits of most of the injection moulding machines that are available, the molecular orientation developed during the mould filling stage is relatively small. On the other hand, the mobility of polymer chains is large, when compared with fibres. Chain relaxation is easy and this leads to an increase in stress relaxation, resulting in a low molecular orientation. In this study, the orientation of pure nylon-6,6 injection moulded parts was investigated, in order to compare their orientation behaviour to that of nylon-6,6 in the composites. The influence of the fibres could therefore be assessed with more certainty.

Orientation measurements, obtained using the 002 reflection, are reported in *Table 3*, whereas a representative scan is reproduced in *Figure 5a*. It can be seen that almost all of the $\langle P_2\rangle$ values are negative. This indicates that the c^*-axis of nylon-6,6 tends to orient perpendicular to the flow direction, with this tendency being increased from the tail to the head zones. A high injection speed aligns the c^*-axis of nylon-6,6 in a direction which is more perpendicular to the flow direction than that

Table 3 Orientation factors $\langle P_2\rangle$ derived from X-ray diffraction measurements for the 002 and 100 reflections of pure injection moulded nylon-6,6

	$\langle P_2\rangle$			
	LSLT	HSLT	LSHT	HSHT
002 Reflection				
Head	−0.175	−0.202	−0.119	−0.226
Centre	−0.082	−0.176	−0.130	−0.170
Tail	0.073	−0.164	0.076	−0.019
100 Reflection				
Head	0.062	0.058	0.067	0.058
Centre	0.046	0.046	0.073	0.063
Tail	0.014	0.036	0.002	−0.021

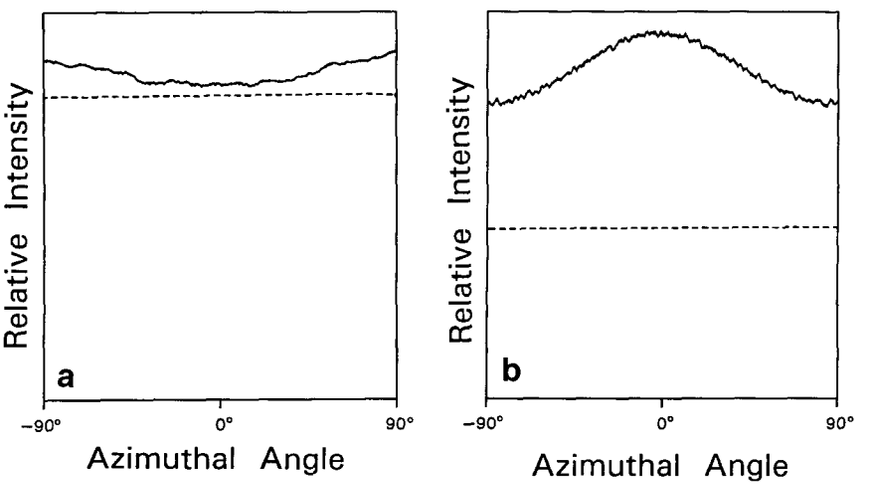

Figure 5 Azimuthal scans of pure, injection moulded nylon-6,6 samples: (a) 002 reflection ($2\theta=12.2°$); (b) 100 reflection ($2\theta=20.3°$)

resulting from a low injection speed at the same mould temperature. In the centre zones and at high injection speeds, mould temperature has little effect on the orientation. This may be due to the 'blunter' velocity profile at high injection speeds. For low injection speeds, high mould temperatures cause the chains to orient perpendicular to the flow direction in a more significant way than that observed for low mould temperatures. This can be attributed to the stronger shear flow effect arising from the thicker solidified layer formed at low mould temperatures.

The bottom half of *Table 3* gives the results of the orientation measurements for the a^*-axis of pure moulded nylon-6,6. A scan of the 100 reflection that is used to ascertain the orientation of the a^*-axis is shown in *Figure 5b*. This axis orients randomly, with the $\langle P_2 \rangle$ values obtained being very close to zero. This indicates that the a^*-axis rotates around the c^*-axis during the growth of crystallites. However, the $\langle P_2 \rangle$ values for a^* show only a modest increase in going from the tail to the head zones. This indicates a slight tendency for this axis to orient in parallel to the flow direction, while the c^*-axis orients markedly in the direction which is perpendicular to the flow direction, as mentioned above.

Orientation of the pultruded composite pellets

It is well known that fibres introduced into the melt of a crystallizable polymer can act as nucleating sites. A transcrystalline layer grows around the fibre in the form of a sheath texture, and crystal orientation in this transcrystalline zone is affected by the presence of the fibres[24].

In order to study the influence of Kevlar fibres on the crystal orientation of the nylon-6,6 matrix, fibre and matrix orientation were measured in composite pellets produced by a pultrusion process. In these pellets, as can be seen by visual inspection, the fibres are well oriented along the pultrusion direction.

Orientation measurements of the 002 reflection of nylon-6,6 are reported in *Figure 6a*. A centring of this reflection is observed at a χ angle of 90°, which indicates that the c^*-axis grows perpendicular to the pultrusion direction. An azimuthal scan of the pellets for the 002 reflection of Kevlar is shown in *Figure 6b*. Two reflections are observed: the one showing the maximum intensity is centred at $\chi = 0°$, while the second reflection, which is centred at $\chi = 90°$, is much broader, indicating a smaller degree of orientation. As discussed above, the 002 reflection of nylon-6,6 can appear with a low intensity on this scan, at the same χ value as its maximum intensity position, as seen in *Figure 6a*. This reflection has been removed from the scan through spectral decomposition prior to calculation of the orientation factor, as described in the Experimental section.

In the composite pellets, an azimuthal angle difference of approximately 90° was found between the fibre axis and the c^*-axis of the matrix. Since the angle between the c^*- and c-axes of nylon-6,6 is $\sim 32°$, it is therefore proposed that, since the c^*-axis is perpendicular to the fibre axis, the chain axis of nylon-6,6 is growing with a tilt angle with respect to the fibre axis. Epitaxial growth could explain this peculiar behaviour: a good match could be established between the a-axis of nylon-6,6 (0.49 nm) and the b-axis of Kevlar (0.518 nm), or twice the value of the a-axis of nylon-6,6 (0.49 nm) and the a-axis of Kevlar (0.787 nm). Unfortunately, because of the various reflection overlaps between Kevlar and nylon-6,6, it is difficult to study the orientation of the a- and b-axes of nylon-6,6. Furthermore, uncertainties concerning the fibre surface structure aggravate the difficulty in investigating in detail the growth of nylon-6,6 crystals on the fibre surface. Therefore, a more thorough study would be necessary to fully understand the epitaxial mechanism of this present system.

Orientation of the injection moulded composites

Orientation in the injection moulded composites was expected to be very different from that of the pultruded samples. However, some striking resemblances were found with respect to the relative orientation of the matrix when compared to that of the fibres.

Orientation measurements obtained for the nylon-6,6 matrix and the Kevlar fibres are reported in *Table 4*. Representative scans of the orientation of nylon-6,6 and Kevlar appear in *Figure 7*. As expected, the 002 reflection of nylon-6,6, which is shown in *Figure 7a*, can also be located in the azimuthal scan of the Kevlar 002 reflection, at a χ angle of 90° in both cases. Again, prior to

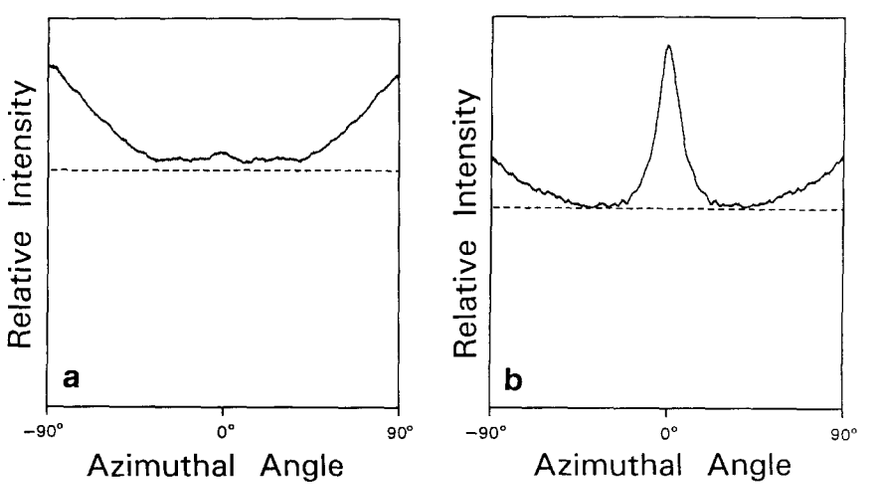

Figure 6 Azimuthal scans of pultruded Kevlar/nylon-6,6 samples used for injection moulding: (a) nylon-6,6, 002 reflection ($2\theta = 12.2°$); (b) Kevlar, 002 reflection ($2\theta = 13.7°$)

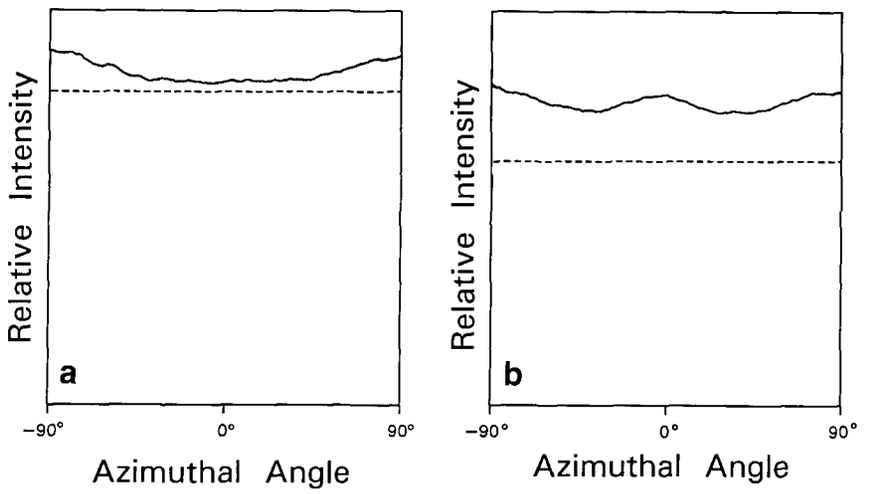

Figure 7 Azimuthal scans of injection moulded composites: (a) nylon-6,6, 002 reflection ($2\theta = 12.2°$); (b) Kevlar, 002 reflection ($2\theta = 13.7°$)

Table 4 Orientation factors $\langle P_2 \rangle$ of composites obtained by X-ray diffraction measurements for the 002 reflections of the Kevlar fibres and the nylon-6,6 matrix

	$\langle P_2 \rangle$			
	LSLT	HSLT	LSHT	HSHT
Kevlar fibres				
Head	−0.007	0.082	−0.022	0.122
Centre	0.292	0.232	0.276	0.246
Tail	0.107	0.198	0.233	0.226
Nylon-6,6 matrix				
Head	−0.028	−0.154	−0.096	−0.117
Centre	−0.162	−0.206	−0.235	−0.238
Tail	0.035	−0.148	−0.129	−0.104

orientation factor calculations, this reflection was removed from the azimuthal scan of the Kevlar 002 reflection.

Most of the $\langle P_2 \rangle$ values for the c^*-axis of nylon-6,6 are negative, with the more negative values being found in the centre zones of the samples. This clearly indicates that the orientation of the c^*-axes of nylon-6,6 tends to be orthogonal to the flow direction. It is interesting to note that the c^*-axis of the nylon-6,6 tends to orient perpendicularly to the flow direction from the tail to the centre zones, whereas it tends to become parallel to the flow direction from the centre to the head zones, which is the exact opposite of what was observed in the fibre orientation behaviour. Moreover, the orientation behaviour of nylon-6,6 in the composites has been found to be quite different from that of pure injection moulded nylon-6,6 samples prepared under the same processing conditions (as reported in *Table 3*). This indicates that the orientation of nylon-6,6 is affected by the presence of the Kevlar fibres, either through interactions between the fibres and the nylon-6,6 molecules, or by changes in the local flow patterns. In fact, during injection moulding of the composites, the cooling procedure begins immediately the melt enters the channel of the mould. Nucleation may be induced by either the local extensional flow or by some of the nucleation sites at the Kevlar fibre surface where the crystallized nylon-6,6 chains anchor. The crystalline growth direction may be determined by both crystal structure matching between the fibres and matrix and the flow conditions near the fibres.

It is interesting to compare differences in the maximum azimuthal angle for both the reflections of the fibres and for the nylon in the centre zones of the composites, moulded under LSLT, HSLT, LSHT, and HSHT processing conditions. This difference is related to the angle between the c-axes of nylon-6,6 and Kevlar in the composites. It takes, respectively, values of 82.0°, 83.9°, 84.0° and 83.6°, which indicates that this difference in the angle remains almost constant, regardless of the moulding conditions. This result corresponds well with that found for the composite pellets where this angle was 90° and supports the hypothesis that the orientation of nylon-6,6 in the composites is largely determined by fibre–matrix interactions, rather than by the local flow conditions. Such a crystalline orientation behaviour of the nylon matrix differs from that presented in the review published by McHugh[25] on the flow-induced crystallization of pure polymers, in which he concluded that nucleation resulted from extensional flow and the crystalline growth direction was dominated by the shear flow. This observation is also different from that of Singh and Kamal[14] concerning the matrix orientation in glass fibre–polypropylene composites, in which they attributed the differences in matrix orientation to the result of molecular relaxation which was restricted by the presence of the fibres. However, the relative fibre volume fractions are smaller (by a factor of two) than those studied here. In the present case, it is believed that the fibre–fibre distance is so small that the relaxation of the matrix is limited and the epitaxial growth of the matrix dominates its orientation.

The $\langle P_2 \rangle$ values measured for Kevlar fibres at the tail, centre, and head zones of the composites are reported in the top part of *Table 4*. It is interesting to note that all of the $\langle P_2 \rangle$ values in the head sections are negative, but are positive in both the centre and tail sections. In all cases, fibre orientation in the flow direction is increased on going from the tail to the centre sections, and decreases from the centre to the head sections.

These observations can be rationalized by referring to the work of Goettler[26] and Owen and Whybrew[27] on short-glass-fibre-filled thermosetting materials, in which they have shown that flow geometry is the major parameter affecting fibre orientation: the orientation changes in the flow channel only if there is a change

in the cross-sectional area. In the tail zone of a dumbbell-shaped cavity, the decrease observed on going from the 'bell' to the 'bone' sections accelerates the fluid (converging flow) and results in a positive velocity gradient. Therefore, fibres tend to rotate in parallel to the line of the flowstream. Because there is no cross-sectional area change in the centre sections, the fibre orientation pattern remains unchanged. In the head zone, where the cavity dimensions increase, the fluid experiences a deceleration (diverging flow), resulting in a negative velocity gradient. Fibres are subjected to a compressional force and rotate perpendicular to the flow direction.

In the centre sections, it has been observed that at both low and high mould temperatures, a low injection speed causes the fibres to orient in the flow direction more significantly than observed with a high injection speed. Two simple rules-of-thumb have been proposed by Tucker[10], namely fibres orient in the flow direction in a simple shear flow and orient in the stretching direction in an elongational flow. However, for short-fibre-reinforced thermoplastics with a high fibre content, it has been shown by Goettler[2] that fibre orientation is more sensitive to elongational flow than to shear flow, due to the blunt velocity profile, and that the rate of fibre rotation is proportional to the value of the normal velocity gradient. The rotation direction is determined by the sign of the velocity gradient. At high injection speeds, the velocity profile is very blunt (almost plug-like). Polymer melt–mould wall contact time is short, which leads to a thin solidified layer. The shear force at the solid–melt interface is therefore lower, inducing fewer fibres to orient in the flow direction. This explains why the fibre orientation patterns remain almost unchanged from those developed previously at the 'gate', where fibres were oriented perpendicular to the flow direction under the influence of a stretching flow perpendicular to the flow direction.

In the case of low injection speeds, where the velocity profiles become less blunt, and the long contact times induce thick solidified layers, the effect of the shear flow, and to a lesser extent of the converging flow, becomes more significant, and fibres align more along the flow direction.

The occurrence of a positive $\langle P_2 \rangle$ value in the head zone under conditions of high injection and high mould temperature can be explained by an even blunter velocity profile, which is not significantly affected by the diverging flow in the head zone. The fibre orientation patterns remain partially the same as those developed at the centre zone.

The Hermans' orientation factors, $\langle P_2 \rangle$, for fibres measured by reflection light microscopy[11] for the centre zones of moulded samples under LSLT, HSLT, LSHT and HSHT conditions were found to be 0.729, 0.615, 0.670 and 0.661, respectively. These values are abnormally high for injection moulding. It is interesting to note that there exists a large difference between these and the $\langle P_2 \rangle$ values obtained by X-ray diffraction, which are reported in *Table 3*. The abnormally high $\langle P_2 \rangle$ values obtained from the Microplan method suggest that this method overestimates the fibre orientation, which is attributed to the preparation method of the samples: the Kevlar fibres, being strong and flexible, are difficult to cut at the microtomed surface, and are pulled out slightly before being cut. This introduces extra fibre orientation at the microtomed surface. However, the $\langle P_2 \rangle$ values obtained from the X-ray diffraction measurements may be slightly underestimated because of the difficulty in accurately measuring the background level. A second factor which is responsible for this underestimation is the incomplete alignment of the PPTA chains with respect to the fibre axis, as reported by Northolt and Van Aartsen[19]. However, interestingly, the orientation factors measured by both methods show a similar trend: increasing the injection speed decreases the fibre orientation in parallel with the flow direction.

CONCLUSIONS

The morphology and orientation of injection moulded short Kevlar fibre/nylon-6,6 composites were found to be related to the processing variables. X-ray diffraction allowed the measurement of both fibre and matrix orientation, on the same portion of a sample, which is not possible with other techniques such as birefringence, contact microradiography, and image analysis. The results indicate that both fibre and matrix orientation exhibit a geometrical dependence. In the centre zones of the moulded samples, an increasing injection speed and mould temperature result in thin skin structure, where fibres orient randomly 'in-plane', and increase the tendency of the fibres to orient perpendicularly to the flow direction in the core region. Low injection speeds and low mould temperatures tend to align the fibres parallel to the flow direction in the core section. Orientation of the matrix is affected by that of the fibres, and this influence is more significant than that of fluid kinematics in determining the matrix orientation. Interactions between fibres and matrix are attributed to epitaxial growth, and consequently to unit cell matching between fibres and matrix.

ACKNOWLEDGEMENTS

The authors wish to acknowledge the financial support of NSERC (National Sciences and Engineering Research Council of Canada), FCAR (Fonds pour la Formation de Chercheurs et l'Aide à la Recherche) and the MESS (action structurante program). We are also indebted to Mr W. Zhang of the Department of Metallurgy, Université Laval, for his help in sawing the moulded samples.

REFERENCES

1 Hegler, R. P. *Kunststoffe* 1984, **74**, 271
2 Goettler, L. A. in 'Mechanical Properties of Reinforced Thermoplastics' (Eds D. W. Clegg and A. A. Collyer), Elsevier, New York, 1986, p. 151
3 Folkes, M. J. 'Short Fibre Reinforced Thermoplastics', Research Studies Press, Chichester, 1982, p. 85
4 Yu, Z., Ait-Kadi, A. and Brisson, J. *Polym. Eng. Sci.* 1991, **31**, 1222
5 Yu, Z., Ait-Kadi, A. and Brisson, J. *Polym. Eng. Sci.* 1991, **31**, 1228
6 Ward, I. M. in 'Advances in Polymer Sciences' (Eds H. H. Kausch and H. G. Zachmann), Vol. 66, Springer, Berlin, 1985, p. 81
7 Darlingtion, M. W. *J. Mater. Sci.* 1975, **10**, 906
8 McGee, S. H. and McCullough, R. L. *J. Appl. Phys.* 1984, **55**, 1394
9 Fischer, G. *Polym. Compos.* 1988, **9**, 297
10 Tucker, C. L. in 'The Manufacturing Science of Composites' (Ed. T. G. Gutowski) Vol. IV, American Society of Mechanical Engineering, New York, 1988, p. 99
11 Yu, Z., Brisson, J. and Ait-Kadi, A. *SPE Tech. Pap.* 1992, **38**, 2663
12 Savitzky, A. and Golay, M. J. E. *Anal. Chem.* 1964, **36**, 1627
13 Bright, P. F., Crowson, R. J. and Folkes, M. J. *J. Mater. Sci.* 1978, **13**, 2497

14 Singh, P. and Kamal, M. R. *Polym. Compos.* 1989, **10**, 344
15 Yu, Z., Brisson, J. and Ait-Kadi, A. *Polym. Compos.* in press
16 Ecochard, F. *J. Chim. Phys. Phys.-Chim.-Biol.* 1946, **43**, 113
17 Bunn, C. W. and Garner, E. V. *Proc. R. Soc. Lond. A* 1947, **189**, 39
18 Lovell, R. and Mitchell, G. R. *Acta Crystallogr. Sect. A* 1981, **37**, 135
19 Northolt, M. G. and Van Aartsen, J. J. *J. Polym. Sci. Polym. Lett. Edn* 1973, **11**, 333
20 Lim, S. H. and White, J. L. *J. Rheol.* 1990, **34**, 343
21 Tadmor, Z. *J. Appl. Polym. Sci.* 1974, **18**, 1753
22 Isayev, A. I. *Polym. Eng. Sci.* 1983, **23**, 271
23 Isayev, A. I. in 'Injection and Compression Molding Fundamentals' (Ed. A. I. Isayev), Marcel Dekker, New York, 1987, p. 283
24 Kumamaru, F., Oono, T., Kajiyama, T. and Takayanagi, M. *Polym. Compos.* 1983, **4**, 141
25 McHugh, A. J. *Polym. Eng. Sci.* 1982, **22**, 15
26 Goettler, L. A. *Modern Plast.* 1970, 140
27 Owen, M. J. and Whybrew, K. *Plast. Rubber* 1976, **1**, 231